

Inhibition of casein kinase 2 sensitizes mantle cell lymphoma to venetoclax through MCL-1 downregulation

Yvonne J. Thus,^{1,2,3} Martin F.M. de Rooij,^{1,2,3} Nathalie Swier,^{1,2,3} Roderick L. Beijersbergen,^{4,5} Jeroen E.J. Guikema,^{1,2,3} Marie-José Kersten,^{2,6} Eric Eldering,^{2,3,7} Steven T. Pals,^{1,2,3} Arnon P. Kater^{2,3,6} and Marcel Spaargaren^{1,2,3}

¹Department of Pathology, Amsterdam UMC, University of Amsterdam; ²Lymphoma and Myeloma Center Amsterdam (LYMMCARE); ³Cancer Center Amsterdam (CCA), Cancer Biology and Immunology – Target & Therapy Discovery; ⁴Division of Molecular Carcinogenesis, Oncode Institute, The Netherlands Cancer Institute; ⁵The NKI Robotics and Screening Center, The Netherlands Cancer Institute; ⁶Department of Hematology, Amsterdam UMC, University of Amsterdam and ⁷Department of Experimental Immunology, Amsterdam UMC, University of Amsterdam, Amsterdam, The Netherlands

Correspondence: M. Spaargaren
marcel.spaargaren@amsterdamumc.nl

Received: June 28, 2022.
Accepted: September 27, 2022.
Early view: October 13, 2022.

<https://doi.org/10.3324/haematol.2022.281668>

©2023 Ferrata Storti Foundation

Published under a CC BY-NC license



SUPPLEMENTARY INFORMATION

Supplementary Methods	<i>Page 2</i>
Figure S1. A kinome-centered synthetic-lethal-screen with venetoclax identifies CK2 KO as potential sensitizer to venetoclax in Z138	<i>Page 8</i>
Figure S2. CK2 is overexpressed and associated with poor prognosis in MCL	<i>Page 10</i>
Figure S3. shRNA-mediated CK2 knock-down sensitizes MCL cells to venetoclax	<i>Page 11</i>
Figure S4. CK2 inhibition by silmitasertib sensitizes MCL cells to venetoclax	<i>Page 12</i>
Figure S5. CK2 inhibition and venetoclax synergize in a cytotoxic manner	<i>Page 15</i>
Figure S6. CK2 regulates MCL-1 protein levels	<i>Page 17</i>
Figure S7. CK2 mediates MCL-1 protein levels via assembly of the translation machinery	<i>Page 18</i>
Figure S8. CK2 inhibition overcomes microenvironmental venetoclax resistance	<i>Page 20</i>
Table S1. Characteristics MCL cell lines	<i>Page 21</i>
Table S2. Primers used for the CRISPR-screen PCR	<i>Page 21</i>
Table S3. Raw counts and gene-based analysis of the kinome-centered CRIPR/Cas9 sensitizer screen	<i>Page 22</i>
Table S4. Primers used for qPCR	<i>Page 23</i>
Table S5. Antibodies used for immunoblotting	<i>Page 24</i>
References	<i>Page 25</i>

SUPPLEMENTAL METHODS

Cell culture and treatment

All cells were cultured with supplement of 10 % fetal calf serum (FCS; Hyclone, GE Healthcare Life Sciences, Pittsburgh PA), 2 mM L-glutamine (Sigma Aldrich), 100 units/mL penicillin (Sigma Aldrich) and 100 µg/mL streptomycin (Sigma Aldrich). Cell lines were routinely authenticated by STR profiling (Promega, Madison, Wisconsin, USA) and monitored for mycoplasma contamination. Each frozen aliquot was used and propagated for no more than 30 passages. For inducible shRNA-mediated knockdown, cells were incubated with 0.5 mM isopropyl β-D-1-thiogalactopyranoside (IPTG) for 3-7 days as indicated.

Patient samples

Peripheral blood derived MCL cells were obtained after routine diagnostics or follow-up procedures at the department of Hematology of the Amsterdam University Medical Centers, location AMC, the Netherlands, and were purified using Ficoll and B cell isolation kit (Milteny Biotec.) Purified MCL samples were sorted on a BD-FACS-Aria IIu to obtain CD5+/CD19+ cells and were cultured on CD40L-expressing L-cells,¹ in IMDM supplemented with 20% fetal calf serum, 2 mM L-glutamine, 100 units/ml penicillin, 100 µg/ml streptomycin, 50 ng/ml IL-10, 50 ng/ml IL-6, 10 ng/ml IGF and 50 ng/ml BAFF. Naïve B-cells (CD19+/IgD+/CD38-) were isolated from tonsil and sorted on a BD FACS-Aria IIu (BD Biosciences).

Transfection, and transduction

Lentiviral particles were produced by transfecting HEK293T cells with pMD2.G (Addgene #12259), pPAX2 (Addgene #12260), and the lentiviral vector in a 1:2:4 ratio with Genius transfection reagent (Westburg, Leusden, the Netherlands) according to the manufacturer's instructions. Three days after transduction, cells were FACS-sorted using a Sony SH800S cell sorter (Sony Biotechnology, San Jose, CA).

Cells transduced with Lenti-Cas9-Blast (Addgene #52962) were selected for 7 days with blasticidin, 24h after transduction. Cas9 activity was analyzed by flow cytometry of Lenti-Cas9-

reporter-transduced cells (Addgene #67980) using the FACSCanto II flow cytometry system (BD Biosciences, San Jose, CA, USA).

Synthetic lethality screen

The screen was performed with the LentiGuide-Puro Brunello kinome library (Addgene #1000000082), which contains 6,204 gRNA constructs targeting 763 different genes, including 100 non-targeting gRNAs.² This library was amplified using ENDURA electrocompetent cells (Lucigen, Middleton, WI) according to manufacturer's instructions. After lentivirus production (see "cloning, transfection, and transduction") and titration, Z138 cells stably expressing Cas9 were transduced in triplicate with a multiplicity of infection (MOI) of 0.3 to ensure transduction with only one gRNA per cells. During the experiment, sufficient cell numbers were transduced and passaged to maintain 1000x coverage of each gRNA to ensure maintenance of the complexity of the library. 24h after transduction, cells were selected for 3 days with 2.5 µg/ml puromycin. Then, 1×10^7 cells were frozen down to serve as a reference (T_0), while another 1×10^7 cells were cultured for 10 population doublings with either 500 nM venetoclax or DMSO before freezing down. Genomic DNA was extracted from cell pellets using Quick DNA miniprep kit (Zymo Research) according to manufacturer's instructions and gRNAs were amplified and labeled using polymerase chain reaction (PCR) amplification.³ Each PCR reaction consisted of 1 µg DNA, 10 µL HF buffer (5x), 1 µL forward primer (10 µM), 1 µL reverse primer (10 µM), 1 µL dNTPs (10 mM), and 0.5 µL Phusion polymerase in a total volume of 50 µL. Barcoded forward primers were used to be able to separate multiplexed samples after next-generation sequencing. PCR program consisted of 2 minutes initial denaturation at 98°C, followed by 21 cycles of 30 seconds denaturation at 98°C, 30 seconds of annealing at 60°C, and 30 seconds elongation at 72°C, and finalized with 5 minutes at 72°C. This PCR reaction was performed 40 times and second PCR reaction was performed, consisting of 2 µl of the pooled first PCR reaction, 10 µL HF buffer (5x), 1 µL forward primer (10 µM), 1 µL reverse primer (10 µM), 1 µL dNTPs (10 mM), and 0.5 µL Phusion polymerase in a total volume of 50 µL. For this reaction a similar PCR program was ran with 15 cycles instead of 21 cycles. Sequences of the used

forward and reverse primers are listed in table S2. PCR product was ran on agarose gel, and purified using the Gel and PCR purification kit (Machery-Nagel) according to manufacturer's protocol, and the abundance of each gRNA was determined by Illumina HiSeq 2500 next-generation sequencing. For sequence depth normalization, total counts of each sample were divided by the geometric mean of all totals. Then, differences in read counts between experimental arms were analyzed using the DeSeq2 and MAGeCK pipeline; the Perl, R, and Python scripts are available at the public GitHub repository (<https://github.com/MFMdeRooij/CRISPRscreen>).^{4,5} Raw data and the list of genes of which their targeting gRNAs are depleted in the venetoclax-treated arm are provided in table S3.

ΔBliss synergy calculation

The ΔBliss synergy score of a combination treatment was calculated by distracting the expected inhibitory effect (I_{Exp}) from the observed inhibitory effect of the drug combination (I_{Obs}). I_{Exp} was calculated by adding up the inhibitory effect of the single treatments (I_{Silm} and I_{Ven}) minus their product: $I_{Silm} + I_{Ven} - I_{Silm} * I_{Ven}$. Thus, ΔBliss synergy score is calculated by: $I_{Obs} - I_{Exp} = I_{Obs} - (I_{Silm} + I_{Ven} - I_{Silm} * I_{Ven})$

RT-qPCR

Total RNA was isolated using TRI-reagent (Sigma-Aldrich), according to the manufacturer's protocol. RNA was converted to cDNA using oligo-dT primers. PCRs were performed using Sensifast (Bioline) on a LightCycler480 RT-PCR detection system and analyzed with LinReg.⁶ Obtained values were normalized to those of the input control β2-microglobulin ($B2M$) and peptidylprolyl isomerase b ($PPIB$). For the sequences of the used primers, see table S4.

Flow cytometry

To assess cell viability, cells were seeded in 96-wells plates and treated as described in figure legends. After treatment, cells were stained with 7-AAD for 10' at room temperature and

measured by flow cytometry on a FACS Cantoll flow cytometer system. Debris and doublets were excluded based upon forward and side scatter profiles. Cell death was established upon the 7-AAD incorporation. Specific cell death was calculated by subtracting the percentage of apoptosis in control cells from the percentage of apoptosis in treated cells. dBliss synergy was calculated with

To determine early apoptosis, cells were stained with Annexin-V-FITC (IQProducts, Groningen, the Netherlands) in Annexin binding buffer (10 mM Hepes, 150 mM NaCl, 5 mM KCl, 1.8 mM CaCl₂, 2.1 mM MgCl₂, 1% glucose, 0.5% BSA) for 15' at 4°C followed by staining with PI (Invitrogen) and analysis on a FACS Cantoll. Debris was excluded based upon forward and side scatter profiles. Early apoptosis was established upon Annexin-V positivity.

To analyze the cell cycle, cells were incubated with 20 µM bromodeoxyuridine (BrdU; Sigma Aldrich) for 1h, washed with ice cold PBS/0.1% BSA and fixed in ice-cold 75% ethanol. The fixed cells were incubated with 0.4 mg/ml pepsin in 2M HCl for 20' at 37°C, followed by 25' incubation with 2M HCl at 37°C. Cells were washed once in PBT (PBS/0.05% Tween-20), and once in PBT_B (PBT/2% BSA) and stained using anti-BrdU FITC (clone B44; BD Bioscience) in PBT_B for 30' at room temperature. After subsequent washing with PBT and PBT_B, cells were treated with 500 µg/ml RNase A (Sigma Aldrich) and stained with 0.1 µM To-Pro-3 (Invitrogen) in PBS/0.1% BSA for 15 minutes at 37°C followed by analysis on a FACS Canto II (BD Biosciences).

Immunoblotting

Cells were lysed in RIPA-buffer (50 mM Tris-HCl pH 7.4, 150 mM NaCl, 1% Nonidet P-40, 0.5% Na-Deoxycholate, 0.1 % Sodium Dodecyl Sulfate), supplemented with protease inhibitor (EDTA-free protease mixture inhibitor; Roche Diagnostics, Rotkreuz, Switzerland) and phosphatase inhibitor (PhosSTOP, Roche Diagnostics). The protein concentration was normalized after performing a bicinchonic acid assay (BCA, Thermo Scientific). 10-15 µg per lysate were separated on Bolt™ 4-12% Bis-Tris Plus gels (Invitrogen) and subsequently blotted to a polyvinylidene fluoride (PVDF)-membrane (Immobilon-P; EMD Millipore,

Burlington, USA). The primary antibodies are listed in table S5. Primary antibodies were detected with anti-mouse-HRP or anti-rabbit-HRP (both DAKO), followed by detection using Pierce™ ECL Western Blotting Substrate (Thermo Scientific). The quantification of the protein bands was assessed using ImageJ software.

The expression of BCL-2 over the combined expression of MCL-1 and BCL-X_L was determined by first correcting the quantified BCL-2, MCL-1 and BCL-X_L protein levels for β-actin levels, followed by normalization of these protein levels to the protein levels in Jeko-1 (normalized to 1) for each protein. These normalized protein levels were used for calculation of the ratio $BCL-2/(MCL-1+BCL-X_L)$.

Microarray analysis

The microarray data of 122 previously untreated MCL patients (GSE93291)⁷, of 43 MCL patients with unspecified clinical history (GSE132929)⁸ and of 10 healthy donor B-cells (GSE28491, E-MTAB-1771), together with the data of 188 CLL patients (GSE31048), 350 DLBCL patients (GSE10846), 67 WM patients (GSE9656), 542 MM patients (GSE2658), 149 FL patients (GSE93261), 59 BL patients (GSE132929) and 23 MZL patients (GSE132929), publically available and deposited in the NIH Gene Expression Omnibus and the EMBL European Bioinformatics Institute databases, were analyzed using the R2 Genomics Analysis and Visualization Platform (r2.amc.nl). The datasets were obtained with the Affymetrix U133p2 array and normalized using the MAS5.0 algorithm.

For Kaplan-Meier analysis, the overall survival of the quartile of MCL patients (GSE93291) with the highest *CSNK2A1*, *CSNK2A2* or *CSNK2B* expression was compared to the quartile of MCL patients with the lowest *CSNK2A1* or *CSNK2B* expression.

Gene Set Enrichment Analysis

Gene Set Enrichment Analysis (GSEA) was performed using the GSEA application (version 4.0.3) on microarray data of 122 MCL patients (GSE93291) comparing the quartile with highest *CSNK2A1* expression to the quartile with lowest *CSNK2A1* expression on the curated

REACTOME and WikiPathway gene sets. GSEA plots were redrawn using the replotGSEA function from the Rtoolbox package (<https://github.com/PeeperLab/Rtoolbox>).

Statistics

Statistical analyses were performed using GraphPad Prism 9 (GraphPad Software, La Jolla, CA). For Kaplan-Meier analysis, log-rank tests were used. For comparisons between 2 groups, 2-tailed Student *t*-tests were performed, for comparisons between more than 2 groups, two-way analysis of variance (ANOVA) with Tukey, Šidák or Dunnett's multiple comparison post-hoc tests were used as indicated in each figure legend. A value of $P < 0.05$ was considered statistically significant. The significance level of *P* values is indicated by asterisks (* $P < 0.05$; ** $P < 0.01$; *** $P < 0.001$; **** $P < 0.0001$; ns, not significant).

SUPPLEMENTARY FIGURE S1

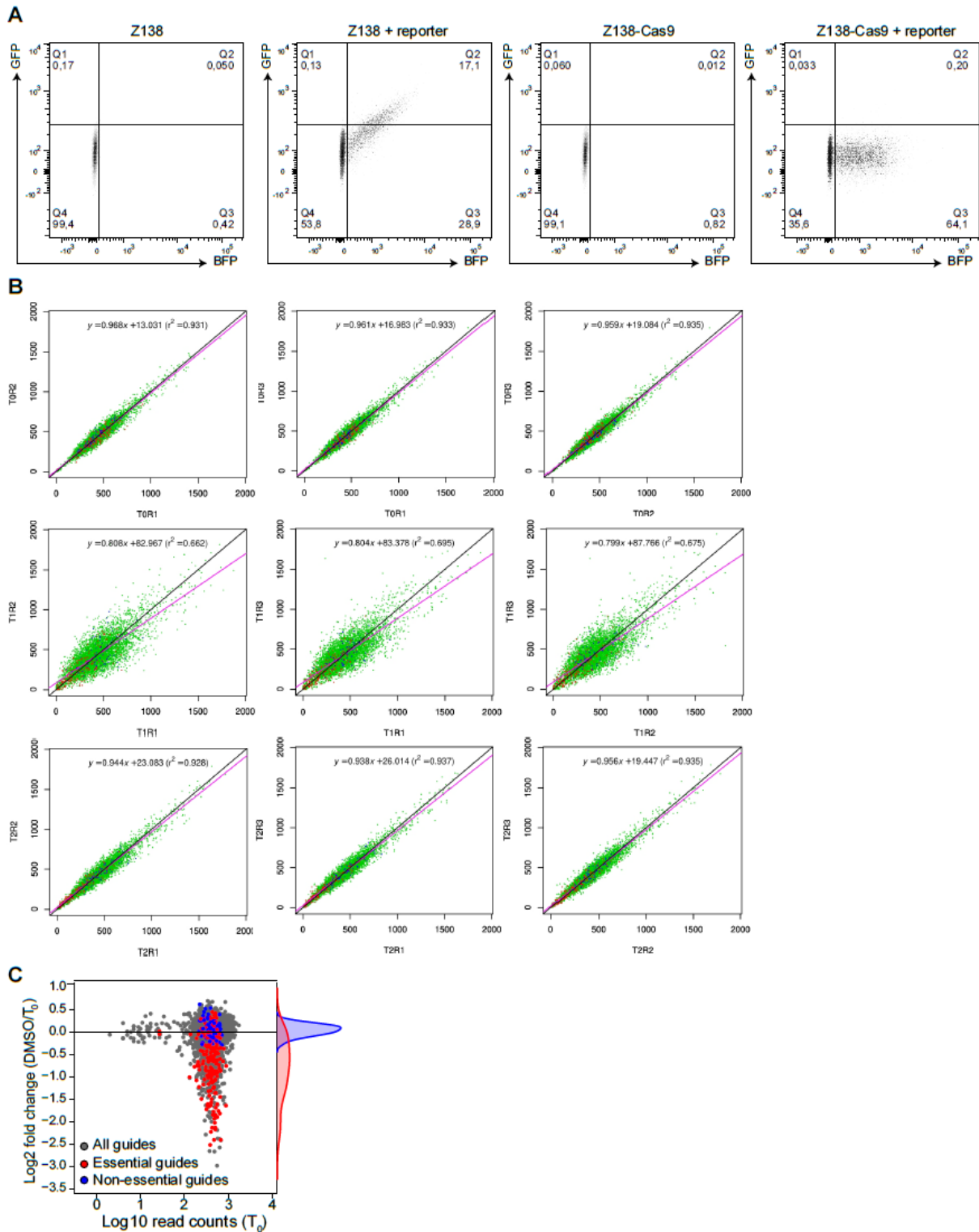
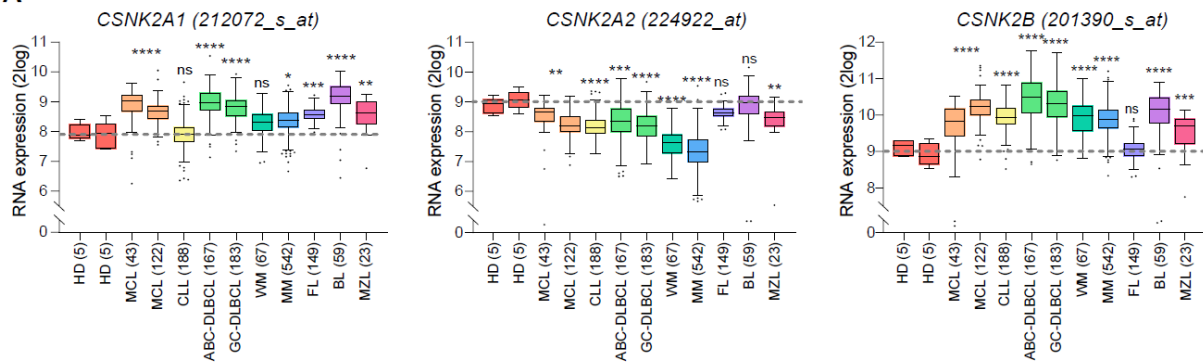


Figure S1. A kinome-centered synthetic-lethal-screen with venetoclax identifies CK2 KO as potential sensitizer to venetoclax in Z138. (A) Flow cytometry plots of parental Z138 cells (two left panels) and Z138 stably expressing Cas9 (two right panels) transduced with a scrambled or Cas9 reporter construct. Cells containing the reporter are BFP positive, GFP

positivity is dependent upon Cas9 activity. (B) Comparisons of sequencing results from the synthetic lethal screen, plotting all gRNA read counts of replicates from T₀ (T0R1-R3, upper row), T₁ DMSO (T1R1-R3, middle row) and T₁ Venetoclax (T2R1-R3, lower row) against each other. (C) Distribution of gRNAs targeting essential genes (red) and non-essential genes (blue) after 10 cell divisions.

SUPPLEMENTARY FIGURE S2

A



B

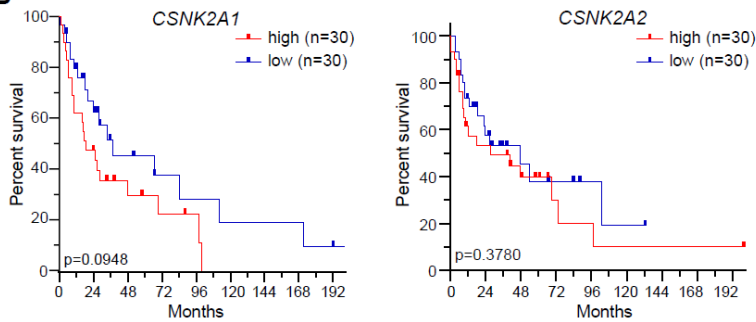


Figure S2. CK2 is overexpressed in MCL and high expression is associated with poor prognosis. (A) mRNA expression of the CK2 subunits in malignant B cells from different B cell lymphomas compared to B cells from healthy donors (HD). Data obtained from publicly available microarray datasets. Between brackets the number of patients per dataset. HD: healthy donor; MCL: mantle cell lymphoma; CLL; chronic lymphocytic leukemia; ABC-DLBCL: activated B-cell type diffuse large B-cell lymphoma; GC-DLBCL: germinal center-type DLBCL; WM: Waldenström macroglobulinemia; MM: multiple myeloma; FL: follicular lymphoma; BL: Burkitt lymphoma; MZL: marginal zone lymphoma. (* $P < 0.05$, ** $P < 0.01$, *** $P < 0.001$, **** $P < 0.0001$, ns: not significant; ANOVA with Dunnett's multiple comparison test). (B) Kaplan-Meier analysis depicting overall survival of patients with MCL from the GSE93291 micro-array dataset divided into the highest and lowest quartile of *CSNK2A1* or *CSNK2A2* expression ($P=0.0948$ and $P=0.3780$ respectively; log-rank test).

SUPPLEMENTARY FIGURE S3

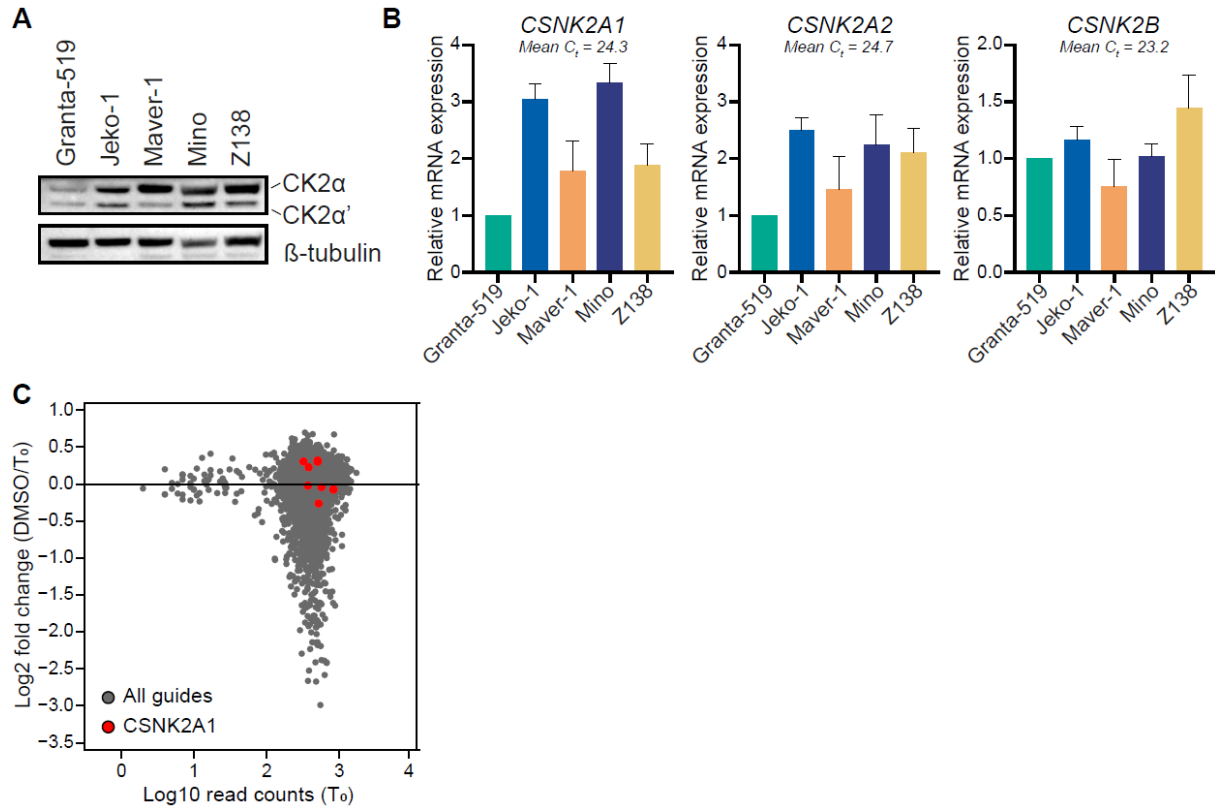
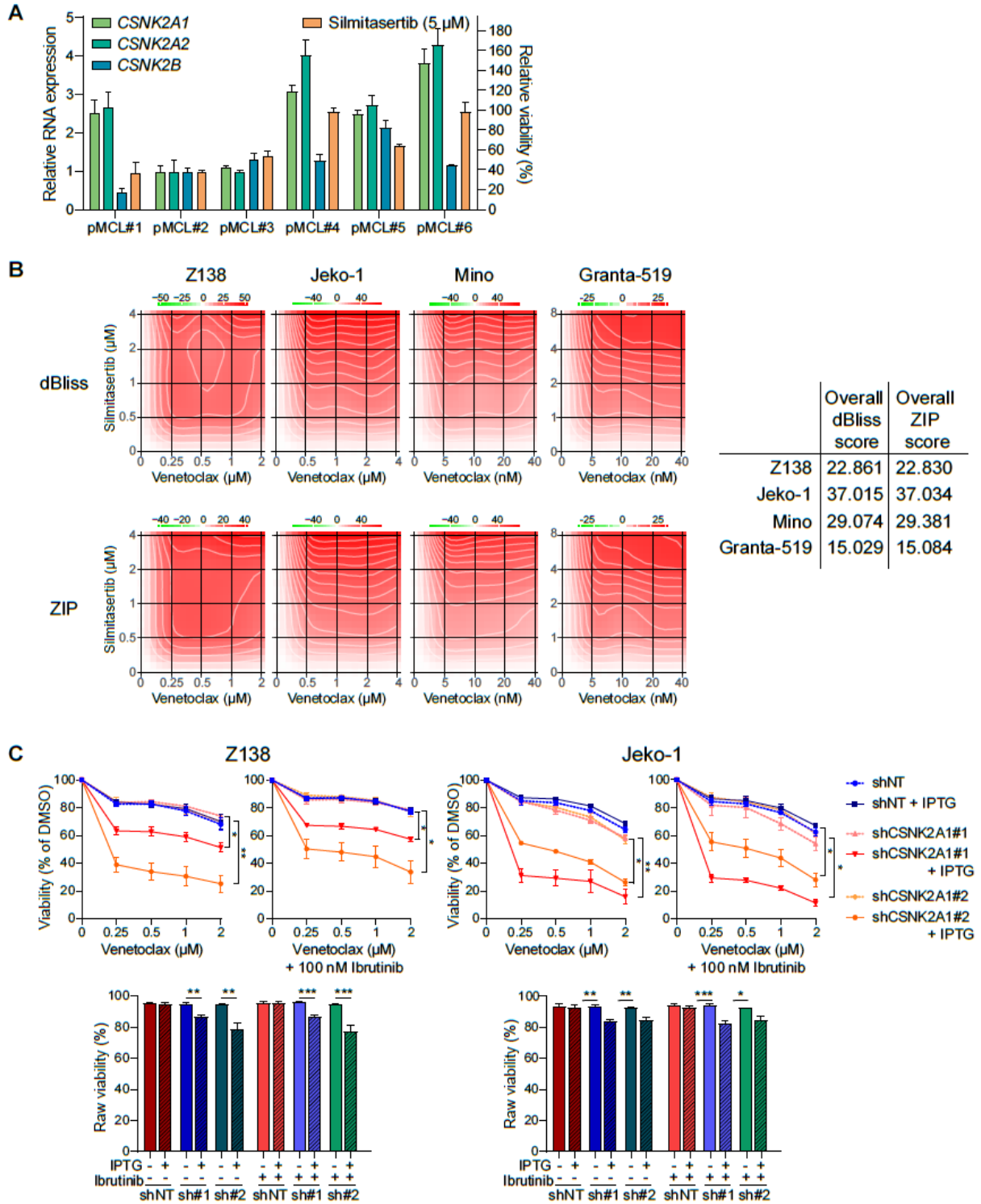


Figure S3. shRNA-mediated CK2 knockdown sensitizes MCL cells to venetoclax. (A) Immunoblot analysis of CK2α and CK2α' protein expression in MCL cell lines. β-tubulin was used as a loading control. Representative immunoblots of three independent experiments are shown. (B) mRNA expression of the CK2 subunits in MCL cell lines as determined by RT-qPCR. *B2M* and *HPRT* were used as input controls. Data are presented as mean +/- SEM of three independent experiments performed in triplicate. (C) The count of the gRNAs from the DMSO treated cells compared to the gRNAs from the T₀ sample depicted in an MA-plot. gRNAs targeting *CSNK2A1* are labeled in red.

SUPPLEMENTARY FIGURE S4



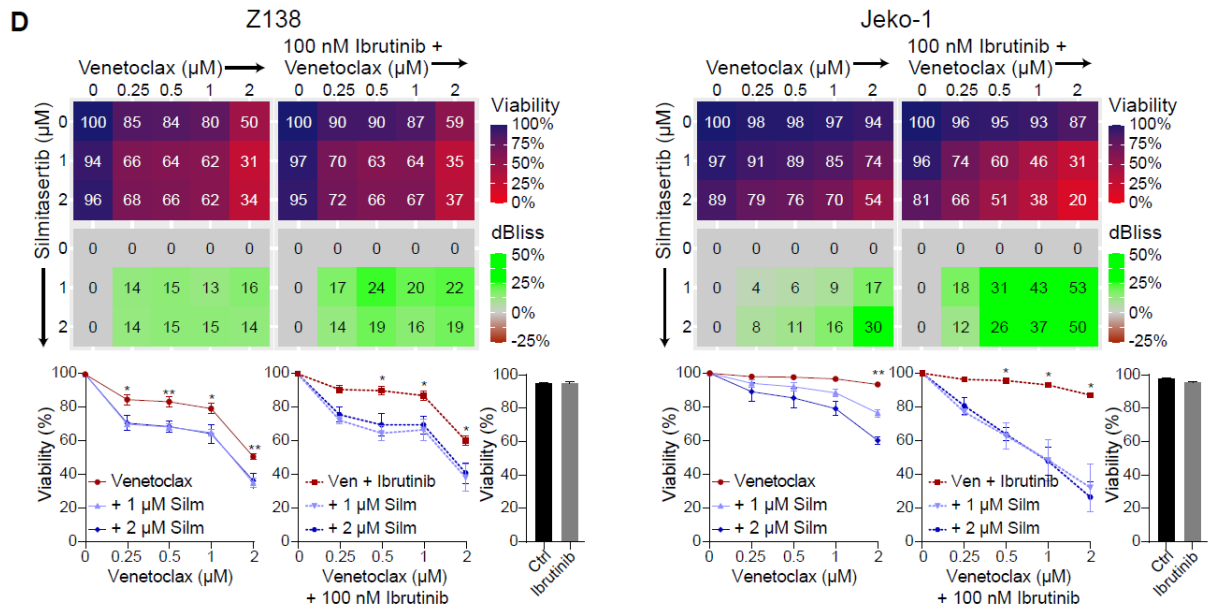


Figure S4. CK2 inhibition by silmitasertib sensitizes MCL cells to venetoclax. (A) mRNA expression of the CK2 subunits in six primary MCL samples as determined by RT-qPCR. *B2M* and *HPRT* were used as input controls. Data are presented as mean \pm SD of a technical triplicate of one experiment (blue/green bars; left y-axis). Flow cytometry analysis of the effect of 2 day treatment with 5 μ M silmitasertib on the viability of 6 primary MCL samples. Data are presented as mean \pm SD of triplicate cultures, relative to untreated samples (orange bars; right y-axis) (B) dBliss and ZIP synergy analysis of the data from figure 4C, as determined by SynergyFinder⁹. (C) Flow cytometry analysis of the effect of venetoclax treatment and venetoclax + ibrutinib treatment on cell viability in *CSNK2A1* KD cells. Cells were treated for 4 days with IPTG, followed by 3 days treatment with both IPTG and venetoclax +/- ibrutinib. The upper panel depicts the percentage viable cells normalized to the condition without venetoclax for each cell line. The lower panel depict the raw percentages of viable cells, and thus the effect of the *CSNK2A1* KD and ibrutinib. The mean \pm SEM of three independent experiments is shown (* P < 0.05, ** P < 0.01; ANOVA with Šidák multiple comparison test). (D) Flow cytometry analysis of the effect of 3 day treatment with venetoclax, silmitasertib, ibrutinib or a combination of these drugs on the cell viability of MCL cell lines Z138 and Jeko-1. The upper panel depicts the percentage viable cells compared to the untreated condition; blue is no effect, red is strong effect. The lower panel depicts the delta-Bliss values; grey is no additional effect,

green is strong synergy. For each cell line, the left panels depict the combination of venetoclax with silmitasertib, the right panels the combination of venetoclax + 100 nM ibrutinib with silmitasertib. The lower panels depict the effect of 3 days venetoclax treatment on cell viability on MCL cell lines treated in combination with different concentrations venetoclax, normalized to the condition without venetoclax exposure. The mean \pm SEM of three independent experiments are shown (* $P < 0.05$, ** $P < 0.01$; ANOVA with Šidák multiple comparison test).

SUPPLEMENTARY FIGURE S5

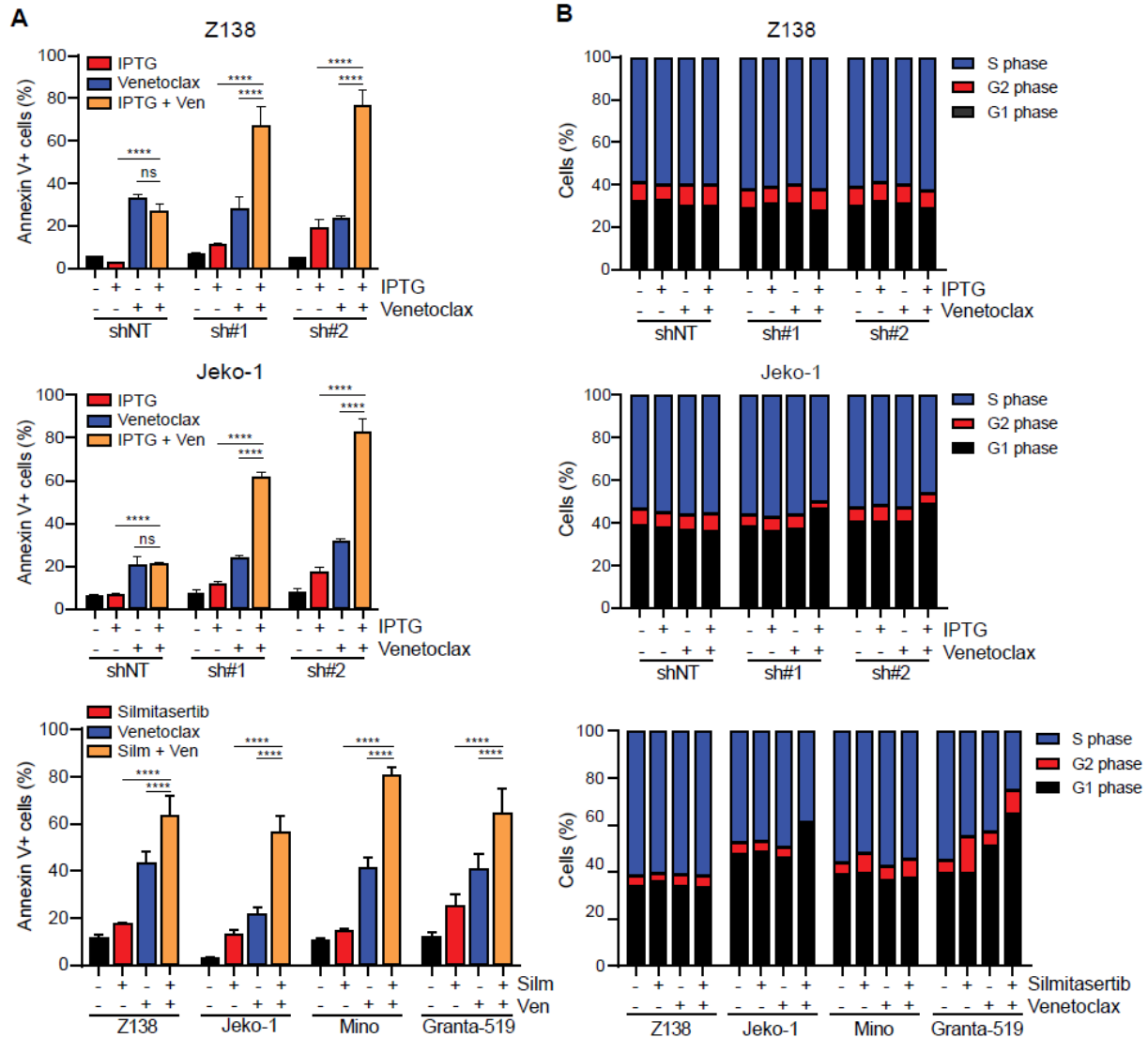


Figure S5. CK2 inhibition and venetoclax exert synergistic cytotoxicity. (A) Apoptosis after CK2 silencing (upper panels) or inhibition (lower panel) in the absence or presence of venetoclax, defined as the percentage of Annexin-V positive cells. Cells expressing shRNAs targeting *CSNK2A1* or a scrambled shRNA (NT) were treated for 4 days with IPTG, followed by three days IPTG treatment in the presence or absence of 0.5 μ M venetoclax. MCL cell lines Z138, Jeko-1, Mino and Granta-519 were treated for three days with 4 μ M silmitasertib in the presence or absence of 1 μ M, 2 μ M, 5 nM and 10 nM venetoclax respectively. Data are presented as mean \pm SEM of three independent experiments (* P < 0.05; ** P < 0.01; *** P < 0.001, **** P < 0.0001; ANOVA with Tukey multiple comparison test). (B) Cell cycle analysis after either CK2 silencing (upper panels) or inhibition (lower panel) in the absence or presence

of venetoclax. Cells expressing shRNAs targeting *CSNK2A1* or a scrambled shRNA (NT) were treated for 4 days with IPTG, followed by three days IPTG treatment in the presence or absence of 1 μ M venetoclax. MCL cell lines Z138, Jeko-1, Mino and Granta-519 were treated for three days with 4 μ M silmitasertib in the presence or absence of 1 μ M, 2 μ M, 5 nM and 10 nM venetoclax respectively. The percentage of cells in G1 (BrdU-, ToPro-3-), G2 (BrdU-, ToPro-3+) and S (BrdU+) phase were determined by flow cytometry analysis. Representative graphs of three independent experiments are shown.

SUPPLEMENTARY FIGURE S6

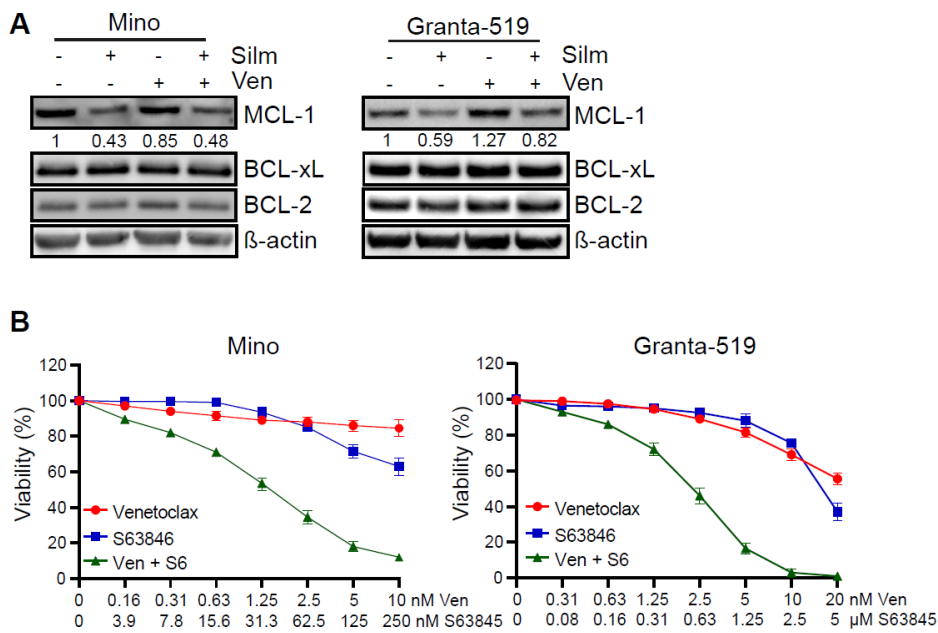


Figure S6. CK2 regulates MCL-1 protein levels. (A) Immunoblot analysis of MCL-1, BCL-X_L and BCL-2 protein expression in Mino and Granta-519 cells pre-treated with 10 μM Q-VD-OPh for 1 hour, followed by 24 hours treatment with 4 μM silmitasertib and or 5 or 10 nM venetoclax respectively. β-actin was used as a loading control. Representative immunoblots of three independent experiments are shown. MCL-1 protein expression is quantified by ImageJ and corrected for β-actin levels. (B) Flow cytometry analysis of the effect of 3 day treatment with indicated concentrations venetoclax, S63845 or the combination of both on the cell viability of MCL cell lines Mino and Granta-519. The mean ± SD of triplicate cultures of a an experiment, representative for at least three independent experiments, is shown.

SUPPLEMENTARY FIGURE S7

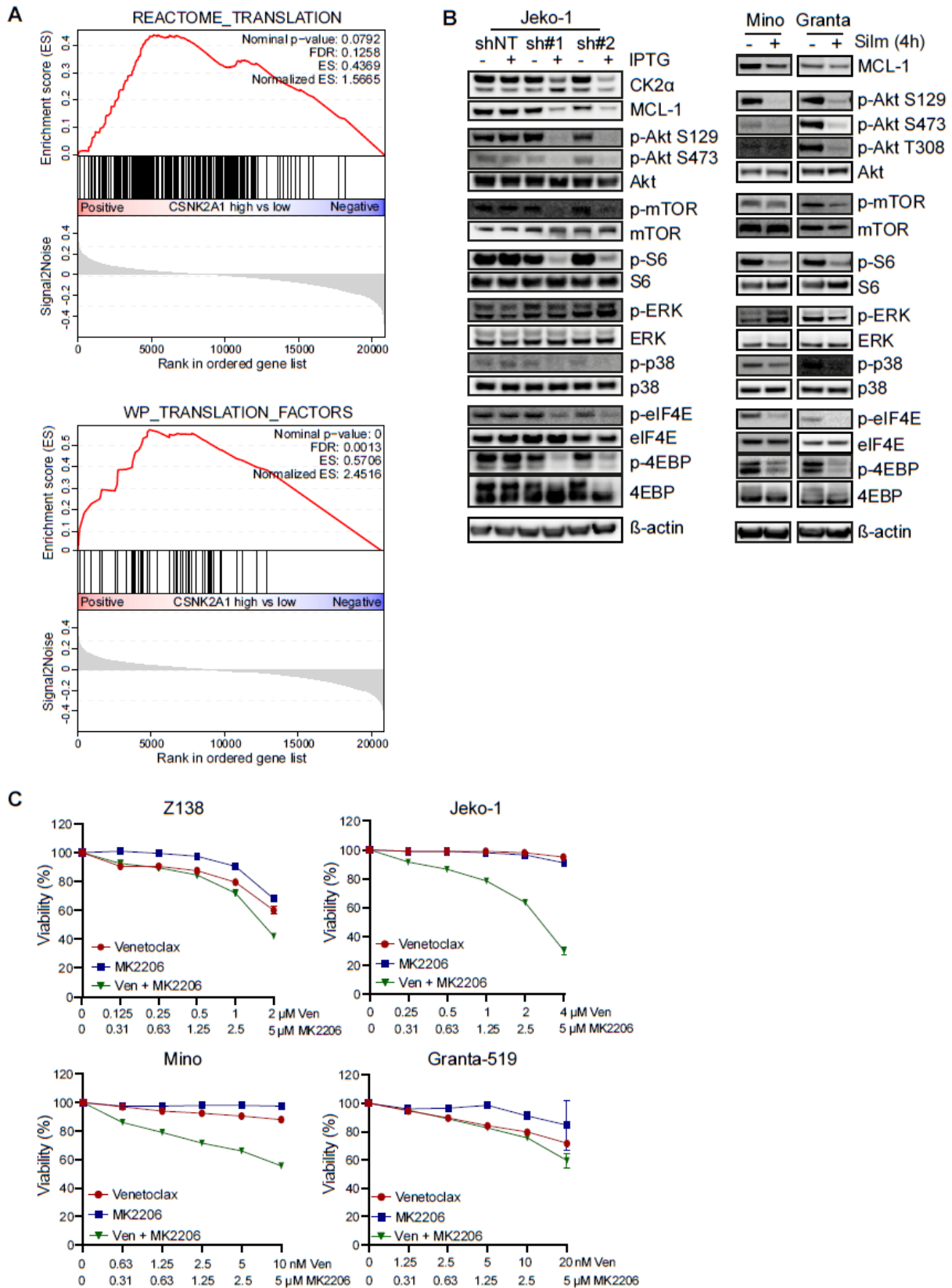


Figure S7. CK2 mediates MCL-1 protein levels via assembly of the translation machinery. (A) Gene Set Enrichment Analysis (GSEA) depicting enrichment of genes

involved in the curated REACTOME gene set Translation and the curated WikiPathways gene set Translation Factors of patients with MCL from the GSE93291 micro-array dataset divided into the highest and lowest quartile of *CSNK2A1* expression. FDR = False Discovery Rate, ES = Enrichment Score. (B) Immunoblot analysis of protein expression of the indicated proteins in Jeko-1 cells expressing two shRNAs targeting *CSNK2A1* or a scrambled shRNA (NT), treated with IPTG for 3 days (left panel) or in Mino and Granta-519 cells pre-treated for 1h with 10 μ M Q-VD-OPh followed by 4h silmitasertib (4 μ M) (right panel). β -actin was used as a loading control. Representative immunoblots of three independent experiments are shown. (C) Flow cytometry analysis of the effect of 3 day treatment with indicated concentrations venetoclax, MK2206 or the combination of both on the cell viability of MCL cell lines Z138, Jeko-1, Mino and Granta-519. The mean \pm SD of triplicate cultures of an experiment, representative for at least three independent experiments, is shown.

SUPPLEMENTARY FIGURE S8

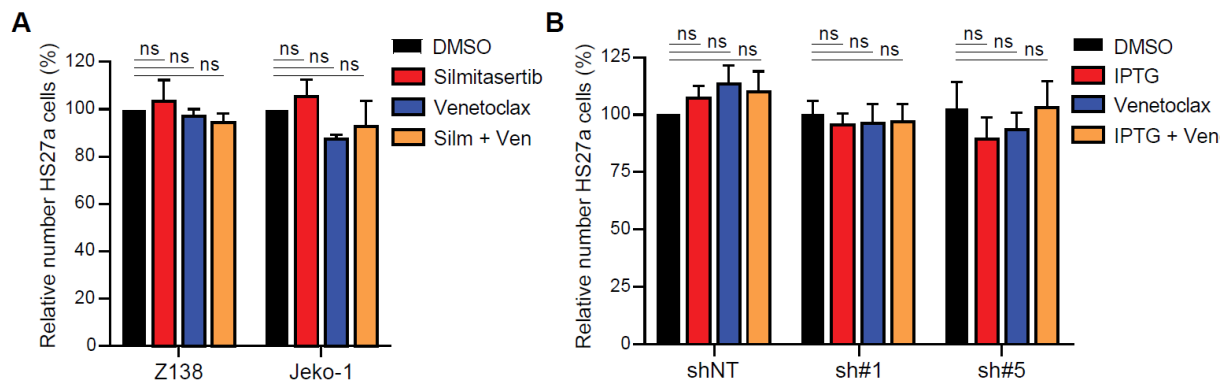


Figure S8. CK2 inhibition overcomes microenvironmental venetoclax resistance. (A)

Flow cytometry analysis of the effect of a 3 day co-culture with Z138 or Jeko-1 on the number of HS27a stromal cells. Cells were treated with either 4 μ M silmitasertib, 1 μ M venetoclax or a combination of both. Data are presented as mean \pm SEM of at least three independent experiments performed in triplicate. (B) Flow cytometry analysis of the effect of a 3 day co-culture with Z138 knock-down cell lines on the number of HS27a stromal cells. Cells were treated with either IPTG, 1 μ M venetoclax or the combination of both. Data are presented as mean \pm SEM of at least three independent experiments performed in triplicate. ns, not significant using two-way ANOVA with Šidák multiple comparison test.

SUPPLEMENTARY TABLES

Table S1 Characteristics MCL cell lines

	Granta-519 ^{10,11}	Jeko-1 ^{11,12}	Maver-1 ^{11,13}	Mino ^{11,14}	Z-138 ^{11,15}
Age	58	78	77	64	70
Gender	F	F	M	M	M
Original diagnosis	MCL	MCL	MCL	MCL	Blastoid MCL
Sample	PB	PB	PB	PB	BM
Cyclin D1	+	+	+	+	++
CD5	-	+	+	+	-
CD23	+	-	-	-	+
EBV	+	-	-	-	-
Ploidy	2N	3N	2N	3N	2N
p53 status	del/wt	del/mut	del/mut	upd/mut	wt
ATM status	del/mut	ampl/*	del/*	wt/*	del/*
p16 ^{INK4A} status	del/del	del/*	del/del	upd/*	del/del
p16 ^{INK4A} expression	-	+	-	+	-
Other	Bcl-2 amp		c-Myc rearrangement		

LN, lymph node; PB, peripheral blood; EBV, Epstein-Barr virus; del, deletion; mut, mutated; wt, wild-type; upd, uniparental disomy; *mutation analysis not performed

Table S2 Primers used for the CRISPR screen PCR

Primer	Sequence
PCR 1 barcoded forward	ACACTCTTTCCCTACACGACGCTCTTCCGATCTXXXXXXXXGGCTTTA TATATCTTGTGGAAAGGACG
PCR 1 reverse	GTGACTGGAGTTCAGACGTGTGCTCTTCCGATCTACTGACGGGCA CCGGAGCCAATTCC
PCR 2 forward	AATGATACGGCGACCACCGAGATCTACACTCTTTCCCTACACGAC GCTCTTCCGATCT
PCR 2 reverse	CAAGCAGAAGACGGCATACGAGATATCACGGTGACTGGAGTTCAG ACGTGTGCTCTTCCGATCT

#	Sample	Barcode
1	T ₀ R1	CGTGAT
2	T ₀ R2	ACATCG
3	T ₀ R3	GCCTAA
4	T _{1-DMSO} R1	TGGTCA
5	T _{1-DMSO} R2	CACTGT
6	T _{1-DMSO} R3	ATTGGC
7	T _{1-Ven} R1	AAGCTA
8	T _{1-Ven} R2	GTAGCC
9	T _{1-Ven} R3	TACAAG

Table S3 Raw counts and gene-based analysis of the kinome-centered CRIPR/Cas9 sensitizer screen.

See supplemental Excel File.

Sheet 1 Raw read counts of the screen. The table shows: (A) sgRNA identifier, (B) target gene symbol, (C) sequence of the gRNA, (D-F) raw counts at day 0 for the three biological replicates, (G-I) raw counts for DMSO-treated samples for the three biological replicates, (J-L) raw counts for venetoclax-treated samples for the three biological replicates.

Sheet 2 List of gene depleted in venetoclax-treated arm. The table shows: (A) target gene symbol, (B) total number of gRNAs targeting each gene, (C) number of gRNAs significantly depleted in venetoclax-treated cells, (D) number of gRNAs significantly enriched in venetoclax-treated cells, (E) minimal fold change of the gRNAs (F) median fold change of the gRNAs (G) maximum fold change of the gRNAs (H) rho depletion score for each gene (I) p-value for depletion in the venetoclax-treated arm for each gene (J) False Discovery Rate for depletion in the venetoclax-treated arm for each gene (K) rho enrichment score in the venetoclax-treated arm for each gene (L) p-value for enrichment in the venetoclax-treated arm for each gene (M) False Discovery Rate for enrichment in the venetoclax-treated arm for each gene

Table S4 Primers used for qPCR

Primer	Sequence
<i>CSNK2A1</i> forward	TGTCCGAGTTGCTTCCCGATACTT
<i>CSNK2A1</i> reverse	TTGCCAGCATACAACCCAAACTCC
<i>CSNK2A2</i> forward	AGCCCACCACCGTATATCAAACCT
<i>CSNK2A2</i> reverse	ATGCTTTCTGGGTCGGGAAGAAGT
<i>CSNK2B</i> forward	TTGGACCTGGAGCCTGATGAAGAA
<i>CSNK2B</i> reverse	TAGCGGGCGTGGATCAATCCATAA
<i>MCL1</i> forward	GTGCCTTTGTGGCTAAACACT
<i>MLC1</i> reverse	AGTCCCGTTTTGTCCTTACGA
<i>PP1B1E</i> forward	AGGCCGGGTGATCTTTGG
<i>PP1B1E</i> reverse	GCTCTTTCCTCCTGTGCCATCTCC
<i>B2M</i> forward	TTTCATCCATCCGACATTG
<i>B2M</i> reverse	CGGCAGGCATACTCATCTTT

Table S5 Antibodies used for immunoblotting

Target	Clone	Number	Manufacturer
MCL-1		ab28147	Abcam, Cambridge, UK
phospho-Akt (Ser129)	EPR6150	ab133458	Abcam
phospho-Akt (Ser473)	D9E XP	4060	Cell Signaling, Beverly, MA
phospho-Akt (Thr308)	D25E6 XP	13038	Cell Signaling
Akt (pan)	C67E7	4691	Cell Signaling
phospho-mTOR (Ser2448)		2971	Cell Signaling
mTOR	7C10	2983	Cell Signaling
phospho-S6 (Ser235/236)	D57.2.2E	4858	Cell Signaling
S6	5G10	2217	Cell Signaling
phospho-4EBP (Thr37/46)	236B4	2885	Cell Signaling
4EBP		9452	Cell Signaling
phospho-eIF4E (Ser209)		9741	Cell Signaling
eIF4E	C46H6	2067	Cell Signaling
phospho-ERK1/2		9101	Cell Signaling
p38		9212	Cell Signaling
BCL-2	124	15071	Cell Signaling
BCL-X _L	54H6	2764	Cell Signaling
phospho-p38 (Thr180)		GTZ78990	GeneTex, Hsinchu, Taiwan
ERK1	C16	sc-093	Santa Cruz, Dallas, TX
CK2 α	1AD9	sc-12738	Santa Cruz
β -actin	AC-15	A5441	Sigma-Aldrich
β -tubulin	D66	T0198	Sigma-Aldrich

REFERENCES

- 1 Garrone P, Neidhardt EM, Garcia E, Galibert L, van Kooten C, Banchereau J. Fas ligation induces apoptosis of CD40-activated human B lymphocytes. *J Exp Med* 1995; 182: 1265–1273.
- 2 Doench JG, Fusi N, Sullender M, Hegde M, Vaimberg EW, Donovan KF *et al.* Optimized sgRNA design to maximize activity and minimize off-target effects of CRISPR-Cas9. *Nat Biotechnol* 2016; 34: 184–191.
- 3 Jastrzebski K, Evers B, Beijersbergen RL. High-throughput RNAi screening. *Methods Mol Biol* 2014; 1470: 183–198.
- 4 Love MI, Huber W, Anders S. Moderated estimation of fold change and dispersion for RNA-seq data with DESeq2. *Genome Biol* 2014; 15: 550.
- 5 Li W, Xu H, Xiao T, Cong L, Love MI, Zhang F *et al.* MAGeCK enables robust identification of essential genes from genome-scale CRISPR/Cas9 knockout screens. *Genome Biol* 2014; 15: 554.
- 6 Ruijter JM, Ramakers C, Hoogaars WMH, Karlen Y, Bakker O, van den Hoff MJB *et al.* Amplification efficiency: linking baseline and bias in the analysis of quantitative PCR data. *Nucleic Acids Res* 2009; 37: e45.
- 7 Scott DW, Abrisqueta P, Wright GW, Slack GW, Mottok A, Villa D *et al.* New Molecular Assay for the Proliferation Signature in Mantle Cell Lymphoma Applicable to Formalin-Fixed Paraffin-Embedded Biopsies. *J Clin Oncol* 2017; 35: 1668–1677.
- 8 Ma MCJ, Tadros S, Bouska A, Heavican T, Yang H, Deng Q *et al.* Subtype-specific and co-occurring genetic alterations in B-cell non-Hodgkin lymphoma. *Haematologica* 2022; 107: 690–701.
- 9 Ianevski A, Giri AK, Aittokallio T. SynergyFinder 2.0: visual analytics of multi-drug combination synergies. *Nucleic Acids Res* 2020; 48: W488–W493.
- 10 Rudolph C, Steinemann D, von Neuhoff N, Gadzicki D, Ripperger T, Drexler HG *et al.* Molecular cytogenetic characterization of the mantle cell lymphoma cell line GRANTA-519. *Cancer Genet Cytogenet* 2004; 153: 144–150.
- 11 Xargay-Torrent S, López-Guerra M, Montraveta A, Saborit-Villarroya I, Rosich L, Navarro A *et al.* Sorafenib inhibits cell migration and stroma-mediated bortezomib resistance by interfering B-cell receptor signaling and protein translation in mantle cell lymphoma. *Clin Cancer Res* 2013; 19: 586–597.
- 12 Jeon HJ, Kim CW, Yoshino T, Akagi T. Establishment and characterization of a mantle cell lymphoma cell line. *Br J Haematol* 1998; 102: 1323–1326.
- 13 Zamò A, Ott G, Katzenberger T, Adam P, Parolini C, Scarpa A *et al.* Establishment of the MAVER-1 cell line, a model for leukemic and aggressive mantle cell lymphoma. *Haematologica* 2006; 91: 40–47.
- 14 Lai R, McDonnell TJ, O'Connor SL, Medeiros LJ, Oudat R, Keating M *et al.* Establishment and characterization of a new mantle cell lymphoma cell line, Mino. *Leuk Res* 2002; 26: 849–855.
- 15 Medeiros LJ, Estrov Z, Rassidakis GZ. Z-138 cell line was derived from a patient with blastoid variant mantle cell lymphoma. *Leuk Res* 2006; 30: 497–501.